Constr. Approx. (2001) 17: 589–617
DOI: 10.1007/s003650010037

CONSTRUCTIVE APPROXIMATION

Approximating the Conformal Maps of Elongated Quadrilaterals by Domain Decomposition

M. I. Falcão, N. Papamichael, and N. S. Stylianopoulos

Abstract. Let $Q := \{\Omega; z_1, z_2, z_3, z_4\}$ be a quadrilateral consisting of a Jordan domain Ω and four points z_1, z_2, z_3, z_4, in counterclockwise order on $\partial\Omega$ and let $m(Q)$ be the conformal module of Q. Then Q is conformally equivalent to the rectangular quadrilateral $\{R_{m(Q)}; 0, 1, 1+im(Q), im(Q)\}$, where $R_{m(Q)} := \{(\xi, \eta) : 0 < \xi < 1, 0 < \eta < m(Q)\}$, in the sense that there exists a unique conformal map $f : \Omega \to R_{m(Q)}$ that takes the four points z_1, z_2, z_3, z_4, respectively, onto the four vertices $0, 1, 1+im(Q), im(Q)$ of $R_{m(Q)}$. In this paper we consider the use of a domain decomposition method (DDM) for computing approximations to the conformal map f, in cases where the quadrilateral Q is "long." The method has been studied already but, mainly, in connection with the computation of $m(Q)$. Here we consider certain recent results of Laugesen [12], for the DDM approximation of the conformal map $f : \Omega \to R_{m(Q)}$ associated with a special class of quadrilaterals (viz., quadrilaterals whose two opposite boundary segments (z_2, z_3) and (z_4, z_1) are parallel straight lines), and seek to extend these results to more general quadrilaterals. By making use of the available DDM theory for conformal modules, we show that the corresponding theory for f can, indeed, be extended to a much wider class of quadrilaterals than those considered by Laugesen.

1. Introduction

Let $Q := \{\Omega; z_1, z_2, z_3, z_4\}$ be a quadrilateral consisting of a Jordan domain Ω and four points z_1, z_2, z_3, z_4, in counterclockwise order on $\partial\Omega$ and let $m(Q)$ be the conformal module of Q. Also, let $R_{m(Q)}$ denote a rectangle of base 1 and height $m(Q)$, i.e.,

$$R_{m(Q)} := \{(\xi, \eta) : 0 < \xi < 1,\ 0 < \eta < m(Q)\}.$$

Then, Q is conformally equivalent to the rectangular quadrilateral

$$\{R_{m(Q)}; 0, 1, 1 + im(Q), im(Q)\},$$

in the sense that there exists a unique conformal map $f : \Omega \to R_{m(Q)}$ that takes the four points z_1, z_2, z_3, z_4, respectively, onto the four vertices $0, 1, 1 + im(Q), im(Q)$ of $R_{m(Q)}$.

This paper is concerned with the study of a domain decomposition method (DDM) for computing approximations to the conformal module $m(Q)$ and the associated conformal

Date received: June 1, 2000. Date accepted: September 6, 2000. Communicated by Dieter Gaier. Online publication: February 26, 2001.
AMS classification: 30C30, 65E05, 30E10, 30C35.
Key words and phrases: Numerical conformal mapping, Quadrilaterals, Domain decomposition.

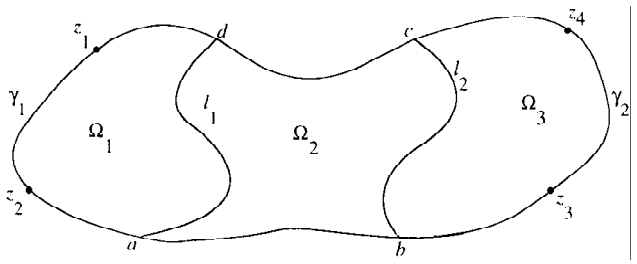

Fig. 1.1

map $f : \Omega \to R_{m(Q)}$, in cases where the quadrilateral Q is long. The method is based on the following three steps:

(i) Decomposing the original quadrilateral $Q := \{\Omega; z_1, z_2, z_3, z_4\}$ (by means of appropriate crosscuts l_j, $j = 1, 2, \ldots$) into two or more component quadrilaterals Q_j, $j = 1, 2, \ldots$; see, e.g., Figure 1.1.

(ii) Approximating the conformal module $m(Q)$ of the original quadrilateral by the sum $\sum_j m(Q_j)$ of the conformal modules of the component quadrilaterals. (Note that

$$m(Q) \geq \sum_j m(Q_j) \tag{1.1}$$

and equality occurs only when the images of all the crosscuts l_j under the conformal map $f : \Omega \to R_{m(Q)}$ are straight lines parallel to the real axis. This follows from the well-known composition law for modules of curve families; see, e.g., [1, pp. 54–56] and [9, pp. 437–438].)

(iii) Approximating the conformal map $f : \Omega \to R_{m(Q)}$, of the original domain Ω, by the conformal maps $f_j : \Omega_j \to R_{m(Q_j)}$ of the subdomains Ω_j, where

$$R_{m(Q_1)} := \{(\xi, \eta) : 0 < \xi < 1,\ 0 < \eta < m(Q_1)\} \tag{1.2}$$

and

$$R_{m(Q_j)} := \left\{(\xi, \eta) : 0 < \xi < 1, \sum_{k=1}^{j-1} m(Q_k) < \eta < \sum_{k=1}^{j} m(Q_k)\right\}, \quad j = 2, 3, \ldots. \tag{1.3}$$

The specific objectives for using the above process are as follows:

(a) To overcome the crowding difficulties associated with the problem of computing the conformal maps of long quadrilaterals, i.e., the difficulties associated with the conventional approach of seeking to determine $m(Q)$ and $f : \Omega \to R_{m(Q)}$ by going via the unit disk or the half-plane (see, e.g., [13, §3.1] and [17, §1]).

(b) To take advantage of the fact that in many applications (e.g., VLSI applications) a complicated original quadrilateral Q can be decomposed into very simple components Q_j (see, e.g., [18, §3] and [19, §4, §5]).

The DDM was introduced by two of the present authors (N.P. and N.S.S.) in [14] and [15], for the purpose of computing the conformal modules and associated conformal maps of a special class of quadrilaterals, viz., quadrilaterals where:

(a) the defining domain Ω is bounded by two parallel straight lines and two Jordan arcs; and
(b) the points z_1, z_2, z_3, z_4 are the four corners where the two boundary arcs meet the two parallel straight lines.

For the same special class of quadrilaterals, the method was also studied by Gaier and Hayman [5], [6], in connection with the computation of conformal modules, and more recently by Laugesen [12], in connection with the determination of the conformal maps. These three papers contain several important results that enhance considerably the associated DDM theory. In particular, the results of Gaier and Hayman provided the necessary tools for extending the application of the DDM to the computation of the conformal modules of a much wider class of quadrilaterals than that considered initially in [14] and [15] (see [16], [17], [18], [19]). The main purpose of the present paper is to investigate the possibility of extending the DDM theory of Laugesen [12], for the conformal map $f : \Omega \to R_{m(Q)}$, to more general quadrilaterals than those having the special form mentioned above.

The paper is organized as follows:

In Section 2 we present a number of preliminary results that are needed for our work in Section 3.

Section 3 contains the main results of the paper. Here, by making use of the theory given in Section 2, we show that Laugesen's DDM theory for the mapping function f can indeed be extended to a much wider class of quadrilaterals than those considered in [12].

Finally, in Section 4 we present several numerical examples illustrating the application of the DDM results obtained in Section 3.

In presenting our results we shall adopt throughout the notations used in [16], [17], [18]. That is:

- Ω and $Q := \{\Omega; z_1, z_2, z_3, z_4\}$ will denote, respectively, the original domain and corresponding quadrilateral.
- $\Omega_1, \Omega_2, \ldots$ and $Q_1, Q_2, \ldots$, will denote, respectively, the "principal" subdomains and corresponding quadrilaterals of the decomposition under consideration.
- The additional subdomains and associated quadrilaterals that arise when the decomposition of Q involves more than one crosscut will be denoted by using (in an obvious manner) a multisubscript notation.

For example, the five component quadrilaterals of the decomposition illustrated in Figure 1.1 are

$$Q_1 := \{\Omega_1; z_1, z_2, a, d\}, \qquad Q_2 := \{\Omega_2; d, a, b, c\}, \qquad Q_3 := \{\Omega_3; c, b, z_3, z_4\},$$

and

$$Q_{1,2} := \{\Omega_{1,2}; z_1, z_2, b, c\}, \qquad Q_{2,3} := \{\Omega_{2,3}; d, a, z_3, z_4\},$$

where

$$\overline{\Omega}_{1,2} := \overline{\Omega}_1 \cup \overline{\Omega}_2, \qquad \overline{\Omega}_{2,3} := \overline{\Omega}_2 \cup \overline{\Omega}_3.$$

2. Preliminary Results

In this section we present a number of preliminary results that are needed for our work in Section 3. The first of these (Lemma 2.1) is a consequence of results given in [12].

Consider a quadrilateral of the form illustrated in Figure 2.1(a), where:

(a) the defining domain Ω is bounded by the straight lines $\Re z = 0$, $\Re z = 1$ and $\gamma_1 := \{z : 0 \le \Re z \le 1,\ \Im z = 0\}$ and a Jordan arc γ_2;
(b) the four points z_1, z_2, z_3, z_4 are the four corners where γ_1 and γ_2 meet the lines $\Re z = 1$ and $\Re z = 0$.

Consider next the decomposition of Q illustrated in the figure, where the crosscut of subdivision is a Jordan arc γ joining the straight lines $\Re z = 0$ and $\Re z = 1$. Also let $R_{m(Q)}$ and $R_{m(Q_2)}$ denote the rectangles

$$R_{m(Q)} := \{(\xi, \eta) : 0 < \xi < 1,\ 0 < \eta < m(Q)\}$$

and

$$R_{m(Q_2)} := \{(\xi, \eta) : 0 < \xi < 1,\ m(Q) - m(Q_2) < \eta < m(Q)\}$$

and let f and f_2 be the associated conformal maps

$$f : \Omega \to R_{m(Q)} \qquad \text{and} \qquad f_2 : \Omega_2 \to R_{m(Q_2)}. \tag{2.1}$$

Lemma 2.1. *With reference to Figure* 2.1 *and the notations introduced above*:

(i)

$$\max_{z \in \gamma_1} |f(z) - z| \le \frac{1}{\pi} \frac{5}{1 - 5e^{-\pi m(Q)}} e^{-\pi m(Q)}, \tag{2.2}$$

provided that $m(Q) > (\log 5)/\pi = 0.512\cdots$.

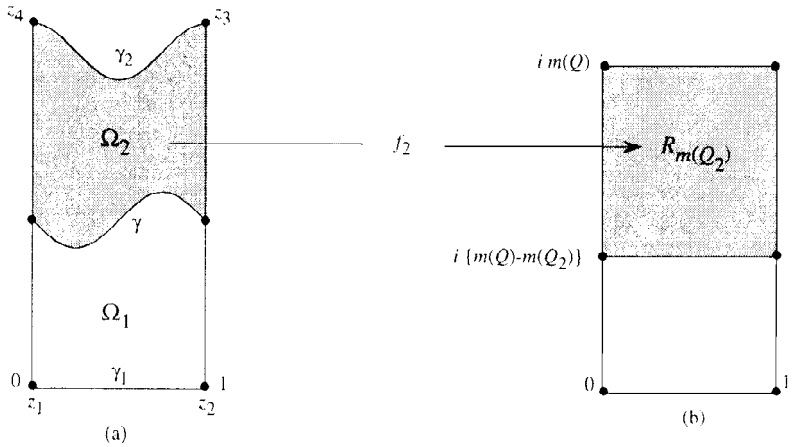

Fig. 2.1

(ii)

$$\max_{z\in\gamma_2} |f(z) - f_2(z)| \le 1.28e^{-\pi m(Q_2)} \tag{2.3}$$

and

$$\max_{z\in\overline{\Omega}_1} |f(z) - z| \le 6.40e^{-\pi m(Q_2)}, \tag{2.4}$$

provided that $m(Q_2) \ge 3$.

(iii) *If the crosscut* γ *is a straight line parallel to the real axis, then*

$$\max_{z\in\gamma_2} |f(z) - f_2(z)| \le 2.57e^{-2\pi m(Q_2)} \tag{2.5}$$

and

$$\max_{z\in\overline{\Omega}_1} |f(z) - z| \le 2.04e^{-\pi m(Q_2)}, \tag{2.6}$$

provided that $m(Q_2) \ge 1$.

Proof. Of the above, Estimates (2.3) and (2.5) can be concluded from the analysis of Laugesen [12], by noting that in our case γ_2 and γ are Jordan arcs and applying Estimate (6.6) of [12, p. 550] to each of the exponential mappings associated with the conformal maps f and f_2. The remaining estimates can be obtained as follows.

The transformation

$$z \to Z := \exp(i\pi z),$$

maps conformally Ω onto the upper half of a symmetric doubly-connected domain G which is bounded externally by the unit circle and internally by a Jordan curve Γ surrounding the origin. Let $1/r$ be the conformal module of G and let g be the function that maps conformally G onto the circular annulus $A := \{W : r < |W| < 1\}$. Then g is related to the mapping function $f : \Omega \to R_{m(Q)}$ by means of

$$g\{\exp(i\pi z)\} = \exp\{i\pi f(z)\} \tag{2.7}$$

and

$$r = \exp\{-\pi m(Q)\}. \tag{2.8}$$

Next, apply the so-called $5r$-theorem of Laugesen [12, p. 535] to the mapping function $g^{-1} : A \to G$, and note that in our case the inner boundary Γ of G is a Jordan curve, to obtain

$$\max_{r\le W\le 1} |g^{-1}(W) - W| < 5r.$$

Therefore,

$$\max_{Z\in\overline{G}} |g(Z) - Z| < 5r.$$

Hence, for any ρ, $e^{-\pi h} \le \rho \le 1$, where $h := \max\{\Im z,\ z \in \gamma\}$:

$$\max_{|Z|=\rho} |\log g(Z) - \log Z| \le \frac{5r}{\rho - 5r}, \tag{2.9}$$

provided $r < \rho/5$; see, e.g., [12, Est. (6.6)]. Estimate (2.2) follows easily from this. It also follows that

$$\max_{z\in\overline{\Omega}_1} |f(z) - z| \le \frac{5e^{-\pi\{m(Q)-h\}}}{\pi(1-5e^{-\pi\{m(Q)-h\}})}, \tag{2.10}$$

provided $m(Q) - h > (\log 5)/\pi = 0.512\cdots$. Further, if $m(Q) - h \ge 1$, then (2.10) gives

$$\max_{z\in\overline{\Omega}_1} |f(z) - z| \le 2.04e^{-\pi\{m(Q)-h\}}.$$

This leads to (2.6), because when γ is a straight line

$$m(Q) \ge m(Q_2) + h.$$

Finally, to obtain estimate (2.4) we make use of the following:

(i) The double inequality

$$h_2 \le m(Q_2) \le h_2 + 1, \tag{2.11}$$

where $h_2 := \min\{\Im z,\ z \in \gamma_2\} - \max\{\Im z,\ z \in \gamma\}$; see [8, pp. 34–37].

(ii) The following two results of Gaier and Hayman (see [5, Theorem 4], [6, Theorems 1, 4], and [16, Theorem 2.1]):

- If $h_2 \ge 2$, then

$$\left| m(Q_2) - h_2 - \frac{1}{\pi}\log r_1 - \frac{1}{\pi}\log r_2 \right| \le 0.381e^{-\pi h_2}, \tag{2.12}$$

where r_1 and r_2 are the so-called exponential radii of the arcs γ and $\overline{\gamma_2}$, respectively. (Here $\overline{\gamma_2}$ denotes the reflection of the arc γ_2 in the real axis.)

- Let $\widehat{Q}$ be the quadrilateral

$$\widehat{Q} := \{\widehat{\Omega}; ih, 1+ih, z_3, z_4\},$$

where $\widehat{\Omega} = \Omega_2 \cap \{z : \Im z > h\}$. Then,

$$-\tfrac{1}{2}0.381e^{-2\pi h_2} \le m(\widehat{Q}) - h_2 - \frac{1}{\pi}\log r_2 \le 0, \tag{2.13}$$

provided $h_2 \ge 1$.

(iii) The two inequalities

$$m(Q) \ge m(\widehat{Q}) + h \qquad \text{and} \qquad r_1 \le 4, \tag{2.14}$$

which result, respectively, from the composition law (1.1) and Koebe's $\frac{1}{4}$-theorem.

Estimate (2.4) follows from (2.10), because (2.11)–(2.14) imply that

$$m(Q) - h > m(Q_2) - 0.441\,983\,4. \qquad \blacksquare$$

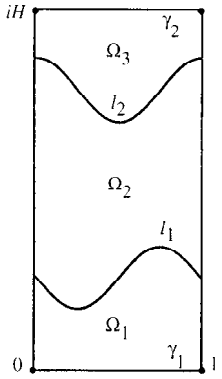

Fig. 2.2

Let Q be the quadrilateral $Q := \{R_H; 0, 1, 1 + iH, iH\}$, where

$$R_H := \{(\xi, \eta) : 0 < \xi < 1,\ 0 < \eta < H\},$$

and consider a decomposition of Q by means of two Jordan arcs l_1 and l_2 as illustrated in Figure 2.2. With the usual notations, let $Q_{1,2}$, Q_2, and $Q_{2,3}$ be the three quadrilaterals that are defined, respectively, by the subdomains $\Omega_{1,2}$, Ω_2, and $\Omega_{2,3}$ and let $R_{m(Q_{1,2})}$, $R_{m(Q_2)}$, and $R_{m(Q_{2,3})}$ be the corresponding conformally equivalent rectangles

$$R_{m(Q_{1,2})} := \{(\xi, \eta) : 0 < \xi < 1,\ 0 < \eta < m(Q_{1,2})\}, \tag{2.15}$$

$$R_{m(Q_2)} := \{(\xi, \eta) : 0 < \xi < 1,\ m(Q_{1,2}) - m(Q_2) < \eta < m(Q_{1,2})\}, \tag{2.16}$$

and

$$R_{m(Q_{2,3})} := \{(\xi, \eta) : 0 < \xi < 1,\ H - m(Q_{2,3}) < \eta < H\}. \tag{2.17}$$

Finally, let $f_{1,2}$, f_2, and $f_{2,3}$ denote the associated conformal maps (see Figure 2.3):

$$f_{1,2} : \Omega_{1,2} \to R_{m(Q_{1,2})}, \qquad f_2 : \Omega_2 \to R_{m(Q_2)}, \qquad f_{2,3} : \Omega_{2,3} \to R_{m(Q_{2,3})},$$

and consider the transformation $T : R_H \to R_H$ defined by

$$T(\zeta) := \begin{cases} f_{2,3}(\zeta), & \text{for } \zeta \in \Omega_3, \\ f_{1,2}(\zeta) + f_{2,3}(\zeta) - f_2(\zeta) & \text{for } \zeta \in \Omega_2, \\ f_{1,2}(\zeta) & \text{for } \zeta \in \Omega_1. \end{cases} \tag{2.18}$$

Note that T is neither continuous across l_1 or l_2, nor a bijective map.

The lemma below says that if R_H is "long," then T is close to the identity map.

Lemma 2.2. *With reference to Figures* 2.2 *and* 2.3, *and the notations introduced above,*

$$E_T := \max_{\zeta \in \overline{R}_H} |T(\zeta) - \zeta| \le 10.39 e^{-\pi m(Q_2)}, \tag{2.19}$$

provided that $m(Q_2) \ge 3$. *If, in addition, the crosscut* l_1 *is a straight line parallel to the real axis* (*so that* $f_{2,3}(\zeta) = \zeta$), *then*

$$E_T \le 4.08 e^{-\pi m(Q_2)}, \tag{2.20}$$

provided that $m(Q_2) \ge 1$.

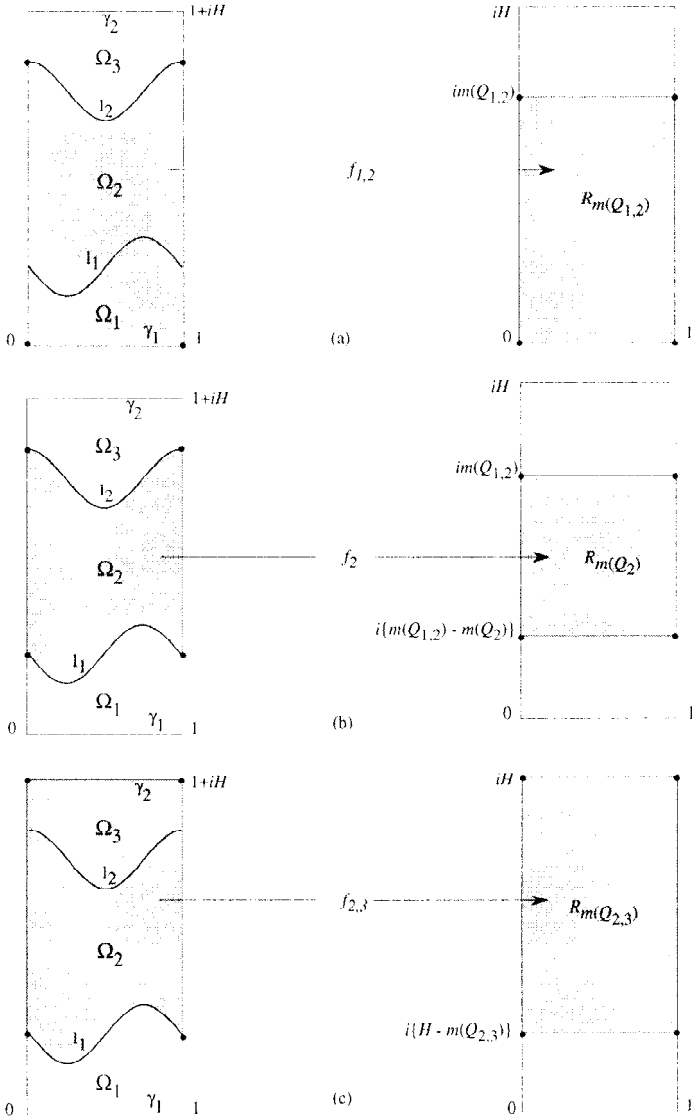

Fig. 2.3

Proof. From (2.18):

$$E_T = \max\left\{\max_{\zeta\in\overline{\Omega}_1}|f_{1,2}(\zeta)-\zeta|,\ \max_{\zeta\in\overline{\Omega}_2}|T(\zeta)-\zeta|,\ \max_{\zeta\in\overline{\Omega}_3}|f_{2,3}(\zeta)-\zeta|\right\}, \tag{2.21}$$

where, from (2.4):

$$\max_{\zeta\in\overline{\Omega}_1}|f_{1,2}(\zeta)-\zeta| \le 6.40e^{-\pi m(Q_2)} \tag{2.22}$$

and

$$\max_{\zeta\in\overline{\Omega}_3} |f_{2,3}(\zeta)-\zeta| \le 6.40e^{-\pi m(Q_2)}, \tag{2.23}$$

provided $m(Q_2)\ge 3$. Further, the function $T(\zeta)-\zeta$ is analytic in Ω_2, continuous on $\overline{\Omega}_2$, and can be extended (by means of the Schwarz reflection principle) to a periodic function, with period 2, in the infinite domain obtained by repeatedly reflecting Ω_2 across its straight-line boundary segments (see, e.g., [7, p. 273]). Therefore, from the maximum modulus principle,

$$\max_{\zeta\in\overline{\Omega}_2} |T(\zeta)-\zeta| = \max\{E_{l_1}, E_{l_2}\}, \tag{2.24}$$

where

$$E_{l_1} := \max_{\zeta\in l_1} |f_{1,2}(\zeta) + f_{2,3}(\zeta) - f_2(\zeta) - \zeta|$$

and

$$E_{l_2} := \max_{\zeta\in l_2} |f_{1,2}(\zeta) + f_{2,3}(\zeta) - f_2(\zeta) - \zeta|.$$

Next, if $m(Q_2)\ge 3$, then from (2.3) and (2.4) we have that

$$\begin{aligned} E_{l_2} &\le \max_{\zeta\in l_2} |f_{1,2}(\zeta) - f_2(\zeta)| + \max_{\zeta\in l_2} |f_{2,3}(\zeta)-\zeta| \\ &\le 1.28e^{-\pi m(Q_2)} + 6.40e^{-\pi m(Q_2)} = 7.68e^{-\pi m(Q_2)} \end{aligned} \tag{2.25}$$

and

$$\begin{aligned} E_{l_1} &\le \max_{\zeta\in l_1} |f_{2,3}(\zeta) - f_2(\zeta) - i\varepsilon_m| + |\varepsilon_m| + \max_{\zeta\in l_1} |f_{1,2}(\zeta)-\zeta| \\ &\le 1.28e^{-\pi m(Q_2)} + |\varepsilon_m| + 6.40e^{-\pi m(Q_2)}, \end{aligned}$$

where

$$\varepsilon_m := H - \{m(Q_{1,2}) + m(Q_{2,3}) - m(Q_2)\}.$$

(The quantity ε_m was introduced in the last estimate, because the function $f_{2,3}$ maps the domain $\Omega_{2,3}$ onto the rectangle $R_{m(Q_{2,3})}$ whose lower side is at a distance $H-m(Q_{2,3})$, rather than $m(Q_{1,2})-m(Q_2)$, from the real axis.) Thus, since from Theorem 2.5 of [19]:

$$|\varepsilon_m| \le 2.71e^{-\pi m(Q_2)},$$

we have that

$$E_{l_1} \le 10.39e^{-\pi m(Q_2)}. \tag{2.26}$$

The required result (2.19) follows from (2.21), by comparing the estimates (2.22)–(2.26).

If l_1 is a straight line parallel to the real axis and $m(Q_2)\ge 1$, then from (2.6):

$$\max_{\zeta\in\overline{\Omega}_1} |f_{1,2}(\zeta)-\zeta| \le 2.04e^{-\pi m(Q_2)}. \tag{2.27}$$

Also, since in this case $f_{2,3}(\zeta) = \zeta$, (2.5) gives

$$E_{l_2} = \max_{\zeta \in l_2} |f_{1,2}(\zeta) - f_2(\zeta)| \leq 2.57 e^{-2\pi m(Q_2)}. \tag{2.28}$$

Finally, from (2.2):

$$\max_{\zeta \in l_1} |f_2(\zeta) - \zeta| \leq 2.04 e^{-\pi m(Q_2)},$$

and hence

$$E_{l_1} \leq \max_{\zeta \in l_1} |f_2(\zeta) - \zeta| + \max_{\zeta \in l_1} |f_{1,2}(\zeta) - \zeta| \leq 4.08 e^{-\pi m(Q_2)}. \tag{2.29}$$

The required result (2.20) follows from (2.21), by comparing the estimates (2.27), (2.28), and (2.29). ■

Consider now a general quadrilateral $Q := \{\Omega; z_1, z_2, z_3, z_4\}$ decomposed as shown in Figure 2.4(a). Let f be the conformal map

$$f : \Omega \to R_{m(Q)} := \{(\xi, \eta) : \ 0 < \xi < 1, \ 0 < \eta < m(Q)\},$$

let $R_{m(Q_{1,2})}$, $R_{m(Q_2)}$, $R_{m(Q_{2,3})}$ denote the rectangles (2.15)–(2.17), with $H = m(Q)$ for $R_{m(Q_{2,3})}$, and let $f_{1,2}$, f_2, and $f_{2,3}$ denote the conformal maps

$$f_{1,2} : \Omega_{1,2} \to R_{m(Q_{1,2})}, \qquad f_2 : \Omega_2 \to R_{m(Q_2)} \qquad \text{and} \qquad f_{2,3} : \Omega_{2,3} \to R_{m(Q_{2,3})}.$$

Also, let $\tilde{f}$ denote the following DDM approximation to f:

$$\tilde{f}(z) := \begin{cases} f_{2,3}(z) & \text{for } z \in \Omega_3, \\ f_{1,2}(z) + f_{2,3}(z) - f_2(z) & \text{for } z \in \Omega_2, \\ f_{1,2}(z) & \text{for } z \in \Omega_1. \end{cases} \tag{2.30}$$

The theorem below may be regarded as the extension of the conformal module Theorem 2.5 of [19], to the case of the conformal map f.

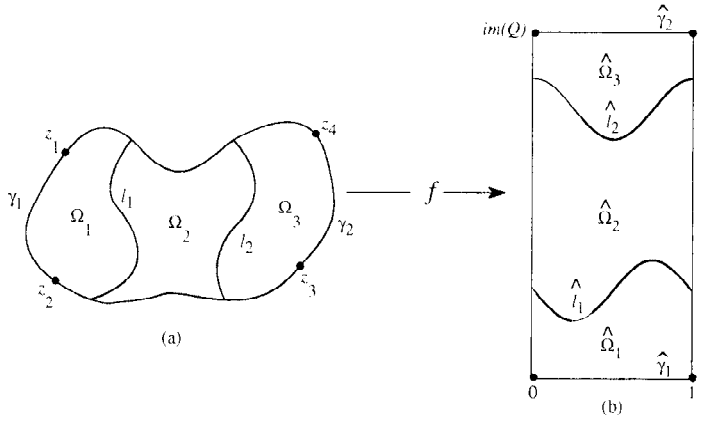

Fig. 2.4

Theorem 2.1. *With reference to Figure* 2.4(a), *let* $\tilde{f}$ *be the DDM approximation* (2.30) *to the conformal map* $f : \Omega \to R_{m(Q)}$. *Then*

$$E_f := \max_{z \in \overline{\Omega}} |f(z) - \tilde{f}(z)| \leq 10.39 e^{-\pi m(Q_2)}, \tag{2.31}$$

provided that $m(Q_2) \geq 3$. *If, in addition, the image of the crosscut* l_1 *under the conformal map* f *is a straight line parallel to the real axis, then*

$$E_f \leq 4.08 e^{-\pi m(Q_2)}, \tag{2.32}$$

provided that $m(Q_2) \geq 1$.

Proof. Let $\widehat{\Omega}_1$, $\widehat{\Omega}_2$, $\widehat{\Omega}_3$, $\hat{l}_1$, $\hat{l}_2$, $\hat{\gamma}_1$, and $\hat{\gamma}_2$ denote, respectively, the images under the conformal map f of Ω_1, Ω_2, Ω_3, l_1, l_2, $\gamma_1 := \widehat{z_1, z_2}$ and $\gamma_2 := \widehat{z_3, z_4}$ (see Figure 2.4), and denote by $\hat{f}_{1,2}$, $\hat{f}_2$, and $\hat{f}_{2,3}$ the conformal maps

$$\hat{f}_{1,2} : \widehat{\Omega}_{1,2} \to R_{m(Q_{1,2})}, \qquad \hat{f}_2 : \widehat{\Omega}_2 \to R_{m(Q_2)} \qquad \text{and} \qquad \hat{f}_{2,3} : \widehat{\Omega}_{2,3} \to R_{m(Q_{2,3})}.$$

Then,

$$f_{1,2}(z) = \hat{f}_{1,2}(f(z)) \quad \text{for } z \in \Omega_{1,2}, \qquad f_2(z) = \hat{f}_2(f(z)) \quad \text{for } z \in \Omega_2,$$

and

$$f_{2,3}(z) = \hat{f}_{2,3}(f(z)) \qquad \text{for} \quad z \in \Omega_{2,3}.$$

Next, let

$$T(\zeta) := \begin{cases} \hat{f}_{2,3}(\zeta) & \text{for } \zeta \in \widehat{\Omega}_3, \\ \hat{f}_{1,2}(\zeta) + \hat{f}_{2,3}(\zeta) - \hat{f}_2(\zeta) & \text{for } \zeta \in \widehat{\Omega}_2, \\ \hat{f}_{1,2}(\zeta) & \text{for } \zeta \in \widehat{\Omega}_1, \end{cases}$$

and observe that for any $z \in \Omega_1 \cup \Omega_2 \cup \Omega_3$, $\tilde{f}(z) = T(\zeta)$, where $\zeta = f(z)$. Thus,

$$E_f = \max_{\zeta \in \overline{R}_{m(Q)}} |T(\zeta) - \zeta|,$$

and the required results follow at once from Lemma 2.2 and the invariance property of conformal modules. ∎

Remark 2.1. With reference to Theorem 2.1, the following estimates hold:

$$\max_{z \in \gamma_1} |f(z) - f_{1,2}(z)| \leq 1.60 e^{-\pi m(Q_{1,2})} \tag{2.33}$$

and

$$\max_{z \in \gamma_2} |f(z) - f_{2,3}(z)| \leq 1.60 e^{-\pi m(Q_{2,3})}, \tag{2.34}$$

provided that $m(Q_2) \geq 3$. This can be seen by observing that

$$\max_{z \in \gamma_1} |f(z) - f_{1,2}(z)| = \max_{\zeta \in \hat{\gamma}_1} |\hat{f}_{1,2}(\zeta) - \zeta|,$$

$$\max_{z \in \gamma_2} |f(z) - f_{2,3}(z)| = \max_{\zeta \in \hat{\gamma}_2} |\hat{f}_{2,3}(\zeta) - \zeta|$$

(see Figure 2.4(b)) and applying Estimate (2.2) to the right-hand side of the last two equations.

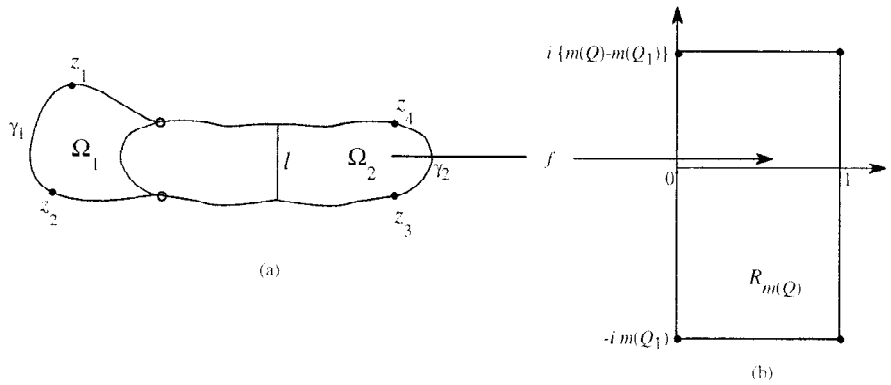

Fig. 3.1

3. DDM for the Conformal Map

The results of this section extend the DDM conformal module results of Theorems 2.4 and 2.6 of [19] to the case of the full conformal map.

Consider a quadrilateral $Q := \{\Omega; z_1, z_2, z_3, z_4\}$ of the form illustrated in Figure 3.1(a), where the defining domain Ω can be decomposed by a straight-line crosscut l into Ω_1 and Ω_2, so that Ω_2 is the reflection in l of some subdomain of Ω_1, as shown in the figure. Let $R_{m(Q)}$, $R_{m(Q_1)}$, and $R_{m(Q_2)}$ be the rectangles

$$R_{m(Q)} := \{(\xi, \eta) : 0 < \xi < 1,\ -m(Q_1) < \eta < m(Q) - m(Q_1)\},$$

$$R_{m(Q_1)} := \{(\xi, \eta) : 0 < \xi < 1,\ -m(Q_1) < \eta < 0\},$$

and

$$R_{m(Q_2)} := \{(\xi, \eta) : 0 < \xi < 1,\ 0 < \eta < m(Q_2)\},$$

and let f_1 and f_2 denote the conformal maps

$$f_1 : \Omega_1 \to R_{m(Q_1)} \qquad \text{and} \qquad f_2 : \Omega_2 \to R_{m(Q_2)}.$$

The theorem below extends the conformal module Theorem 2.4 of [19] to the case of the conformal map f.

Theorem 3.1. *With reference to Figure* 3.1, *and the notations introduced above,*

$$E_f^{\{1\}} := \max_{z \in \overline{\Omega}_1} |f(z) - f_1(z)| \le 2.04 e^{-\pi m(Q_2)} \tag{3.1}$$

and

$$E_f^{\{2\}} := \max_{z \in \overline{\Omega}_2} |f(z) - f_2(z)| \le 4.08 e^{-\pi m(Q_2)}, \tag{3.2}$$

provided that $m(Q_2) \ge 1$.

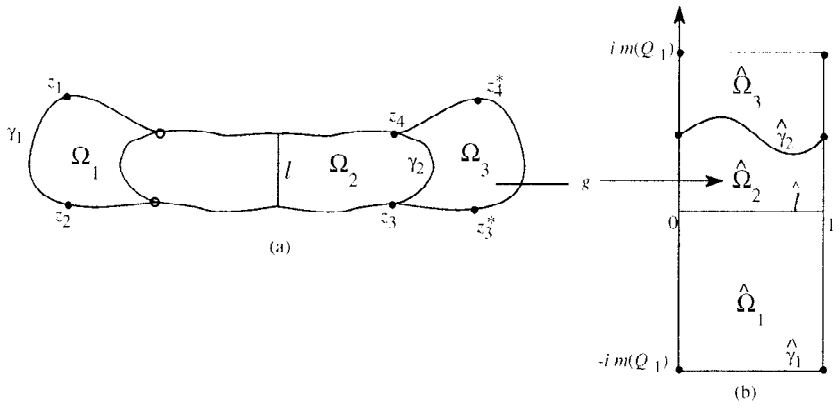

Fig. 3.2

Proof. Reflect Ω_1 in l and consider the decomposition of the resulting quadrilateral $Q^* := \{\Omega^*; z_1, z_2, z_3^*, z_4^*\}$ illustrated in Figure 3.2(a). Then the symmetry of Q^* implies that $m(Q^*) = 2m(Q_1)$ and that the image of the crosscut l, under the conformal map

$$g : \Omega^* \to R_{m(Q^*)} := \{(\xi, \eta) : 0 < \xi < 1,\ -m(Q_1) < \eta < m(Q_1)\},$$

is the segment $\widehat{l} := \{(\xi, 0) : 0 \le \xi \le 1\}$ of the real axis.

Let $\widehat{\Omega}_1$, $\widehat{\Omega}_2$, $\widehat{\Omega}_3$, $\widehat{\gamma}_1$, $\widehat{\gamma}_2$ be the images, under g, of Ω_1, Ω_2, Ω_3, $\gamma_1 := \widehat{z_1, z_2}$, and $\gamma_2 := \widehat{z_3, z_4}$ (see Figure 3.2), and consider the conformal maps

$$\widehat{g}_1 : \widehat{\Omega}_1 \to R_{m(Q_1)}, \qquad \widehat{g}_2 : \widehat{\Omega}_2 \to R_{m(Q_2)} \qquad \text{and} \qquad \widehat{g}_{1,2} : \widehat{\Omega}_{1,2} \to R_{m(Q)}.$$

Then,

$$f_1(z) = \widehat{g}_1(g(z)), \quad z \in \Omega_1, \qquad f_2(z) = \widehat{g}_2(g(z)), \quad z \in \Omega_2,$$

and

$$f(z) = \widehat{g}_{1,2}(g(z)), \qquad z \in \Omega.$$

That is,

$$f_1(z) = \widehat{g}_1(\zeta) = \zeta, \qquad f_2(z) = \widehat{g}_2(\zeta) \qquad \text{and} \qquad f(z) = \widehat{g}_{1,2}(\zeta),$$

where $\zeta = g(z)$. Therefore, from (2.6):

$$E_f^{\{1\}} = \max_{\zeta \in \widehat{\widehat{\Omega}}_1} |\widehat{g}_{1,2}(\zeta) - \zeta| \le 2.04 e^{-\pi m(Q_2)}. \tag{3.3}$$

Also, by applying to $\widehat{g}_{1,2}(\zeta) - \widehat{g}_2(\zeta)$ the argument used for the function $T(\zeta) - \zeta$ at the beginning of the proof of Lemma 2.2, we find that

$$E_f^{\{2\}} = \max_{\zeta \in \widehat{\widehat{\Omega}}_2} |\widehat{g}_{1,2}(\zeta) - \widehat{g}_2(\zeta)| = \max\{E_{\widehat{l}}, E_{\widehat{\gamma_2}}\}, \tag{3.4}$$

where

$$E_{\widehat{I}} := \max_{\zeta \in \widehat{I}} |\widehat{g}_{1,2}(\zeta) - \widehat{g}_2(\zeta)| \qquad \text{and} \qquad E_{\widehat{\gamma}_2} := \max_{\zeta \in \widehat{\gamma}_2} |\widehat{g}_{1,2}(\zeta) - \widehat{g}_2(\zeta)|.$$

Next, by using (2.2) and (2.6):

$$\begin{aligned} E_{\widehat{I}} &\leq \max_{\zeta \in \widehat{I}} |\widehat{g}_2(\zeta) - \zeta| + \max_{\zeta \in \widehat{I}} |\widehat{g}_{1,2}(\zeta) - \zeta| \\ &\leq 4.08 e^{-\pi m(Q_2)}. \end{aligned} \tag{3.5}$$

Also, from (2.5):

$$\begin{aligned} E_{\widehat{\gamma}_2} &\leq \max_{\zeta \in \widehat{\gamma}_2} |\widehat{g}_{1,2}(\zeta) - \widehat{g}_2(\zeta) - i\varepsilon_m| + \varepsilon_m \\ &\leq 2.57 e^{-2\pi m(Q_2)} + \varepsilon_m, \end{aligned} \tag{3.6}$$

where the quantity

$$\varepsilon_m := m(Q) - \{m(Q_1) + m(Q_2)\} \tag{3.7}$$

is introduced in (3.6), because the function $\widehat{g}_{1,2}$ maps the domain $\widehat{\Omega}_{1,2}$ onto the rectangle $R_{m(Q)}$ whose upper side is at a distance $m(Q) - m(Q_1)$, rather than $m(Q_2)$, from the real axis. Thus, since from [19, Theorem 2.4]:

$$0 \leq \varepsilon_m \leq \frac{4}{\pi} e^{-2\pi m(Q_2)},$$

we have that

$$E_{\widehat{\gamma}_2} \leq 3.85 e^{-2\pi m(Q_2)}. \tag{3.8}$$

Therefore, from (3.4), (3.5), and (3.8):

$$E_f^{\{2\}} \leq 4.08 e^{-\pi m(Q_2)}. \qquad \blacksquare$$

Remark 3.1. With reference to Theorem 2.1, the following estimates hold, provided $m(Q_2) \geq 1$:

$$\max_{z \in \gamma_1} |f(z) - f_1(z)| \leq 2.04 e^{-\pi m(Q)} \tag{3.9}$$

and

$$\max_{z \in \gamma_2} |f(z) - f_2(z)| \leq 3.85 e^{-2\pi m(Q_2)}. \tag{3.10}$$

These follow at once from (2.2) and (3.8), because

$$\max_{z \in \gamma_1} |f(z) - f_1(z)| = \max_{\zeta \in \widehat{\gamma}_1} |\widehat{g}_{1,2}(\zeta) - \zeta|$$

and

$$\max_{z \in \gamma_2} |f(z) - f_2(z)| = \max_{\zeta \in \widehat{\gamma}_2} |\widehat{g}_{1,2}(\zeta) - \widehat{g}_2(\zeta)| =: E_{\widehat{\gamma}_2}.$$

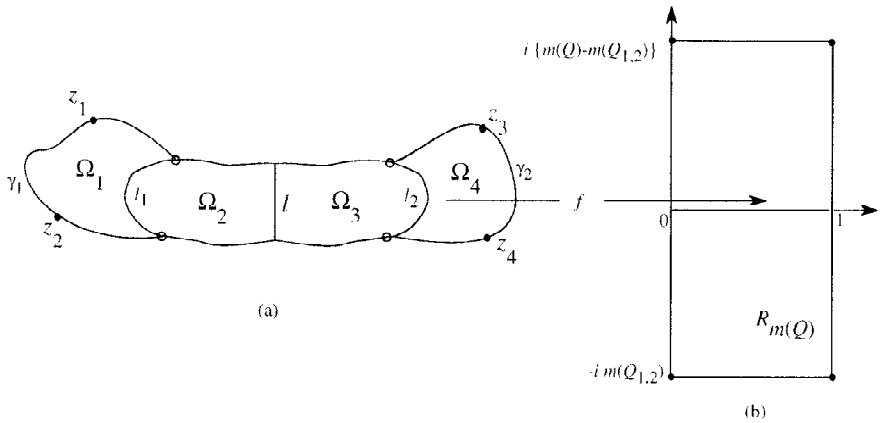

Fig. 3.3

Consider now a quadrilateral $Q := \{\Omega; z_1, z_2, z_3, z_4\}$ of the form illustrated in Figure 3.3(a), where the defining domain Ω can be decomposed by means of a straight-line crosscut l and two other crosscuts l_1 and l_2 into four subdomains Ω_1, Ω_2, Ω_3, and Ω_4, so that Ω_3 is the reflection in l of Ω_2. Let

$$\begin{aligned} R_{m(Q)} &:= \{(\xi,\eta) : 0 < \xi < 1,\ -m(Q_{1,2}) < \eta < m(Q) - m(Q_{1,2})\},\\ R_{m(Q_{1,2})} &:= \{(\xi,\eta) : 0 < \xi < 1,\ -m(Q_{1,2}) < \eta < 0\},\\ R_{m(Q_{3,4})} &:= \{(\xi,\eta) : 0 < \xi < 1,\ 0 < \eta < m(Q_{3,4})\} \end{aligned}$$

and denote by f the conformal map $f : \Omega \to R_{m(Q)}$ and by $\tilde{f}$ the following DDM approximation to f:

$$\tilde{f}(z) := \begin{cases} f_{3,4}(z) : \Omega_{3,4} \to R_{m(Q_{3,4})}, \\ f_{1,2}(z) : \Omega_{1,2} \to R_{m(Q_{1,2})}. \end{cases} \tag{3.11}$$

The theorem below extends the conformal module Theorem 2.6 of [19] to the case of the full conformal map f.

Theorem 3.2. *With reference to Figure* 3.3, *and the notations introduced above,*

$$E_f := \max_{z\in\overline{\Omega}} |f(z) - \tilde{f}(z)| \le 6.17 e^{-\pi m(Q_2)}, \tag{3.12}$$

provided that $m(Q_2) \ge 1.5$.

Proof. Recall that

$$f : \Omega \to R_{m(Q)} := \{(\xi,\eta) : 0 < \xi < 1,\ -m(Q_{1,2}) < \eta < m(Q) - m(Q_{1,2})\},$$

let

$$\begin{aligned} R_{m(Q_{1,2,3})} &:= \{(\xi,\eta) : 0 < \xi < 1,\ -m(Q_{1,2}) < \eta < m(Q_{1,2,3}) - m(Q_{1,2})\},\\ R_{m(Q_{2,3})} &:= \{(\xi,\eta) : 0 < \xi < 1,\\ &\qquad m(Q_{1,2,3}) - m(Q_{1,2}) - m(Q_{2,3}) < \eta < m(Q_{1,2,3}) - m(Q_{1,2})\},\\ R_{m(Q_{2,3,4})} &:= \{(\xi,\eta) : 0 < \xi < 1,\\ &\qquad m(Q) - m(Q_{1,2}) - m(Q_{2,3,4}) < \eta < m(Q) - m(Q_{1,2})\}, \end{aligned}$$

and consider the transformation

$$g(z) := \begin{cases} f_{2,3,4}(z) & \text{for } z \in \Omega_4,\\ f_{1,2,3}(z) + f_{2,3,4}(z) - f_{2,3}(z) & \text{for } z \in \Omega_{2,3},\\ f_{1,2,3}(z) & \text{for } z \in \Omega_1, \end{cases}$$

where

$$f_{1,2,3} : \Omega_{1,2,3} \to R_{m(Q_{1,2,3})}, \qquad f_{2,3} : \Omega_{2,3} \to R_{m(Q_{2,3})}, \qquad f_{2,3,4} : \Omega_{2,3,4} \to R_{m(Q_{2,3,4})},$$

(see Figure 3.4). Then, from Theorem 2.1 (Estimate (2.31)) we have that

$$\max_{z\in\overline{\Omega}} |f(z) - g(z)| \le 10.39 e^{-2\pi m(Q_2)}, \tag{3.13}$$

provided $m(Q_2) \ge 1.5$. (Note that because of the symmetry $m(Q_{2,3}) = 2m(Q_2)$.)

Our next objective is to estimate $\max_{z\in\overline{\Omega}} |g(z) - \tilde{f}(z)|$. We do this by estimating separately the errors

$$E_g^{\{j\}} := \max_{z\in\overline{\Omega}_j} |g(z) - \tilde{f}(z)|, \qquad j = 1,2,3,4,$$

as follows:

(i)

$$E_g^{\{1\}} = \max_{z\in\overline{\Omega}_1} |f_{1,2,3}(z) - f_{1,2}(z)|.$$

Therefore, from (3.1):

$$E_g^{\{1\}} \le 2.04 e^{-\pi m(Q_2)}, \tag{3.14}$$

provided $m(Q_2) \ge 1$.

(ii)

$$\begin{aligned} E_g^{\{2\}} &= \max_{z\in\overline{\Omega}_2} |f_{1,2,3}(z) + f_{2,3,4}(z) - f_{2,3}(z) - f_{1,2}(z)| \\ &\le \max_{z\in\overline{\Omega}_2} |f_{1,2,3}(z) - f_{1,2}(z)| + \max_{z\in\overline{\Omega}_2} |f_{2,3,4}(z) - f_{2,3}(z)|, \end{aligned} \tag{3.15}$$

where, from (3.1):

$$\max_{z\in\overline{\Omega}_2} |f_{1,2,3}(z) - f_{1,2}(z)| \le 2.04 e^{-\pi m(Q_2)}, \tag{3.16}$$

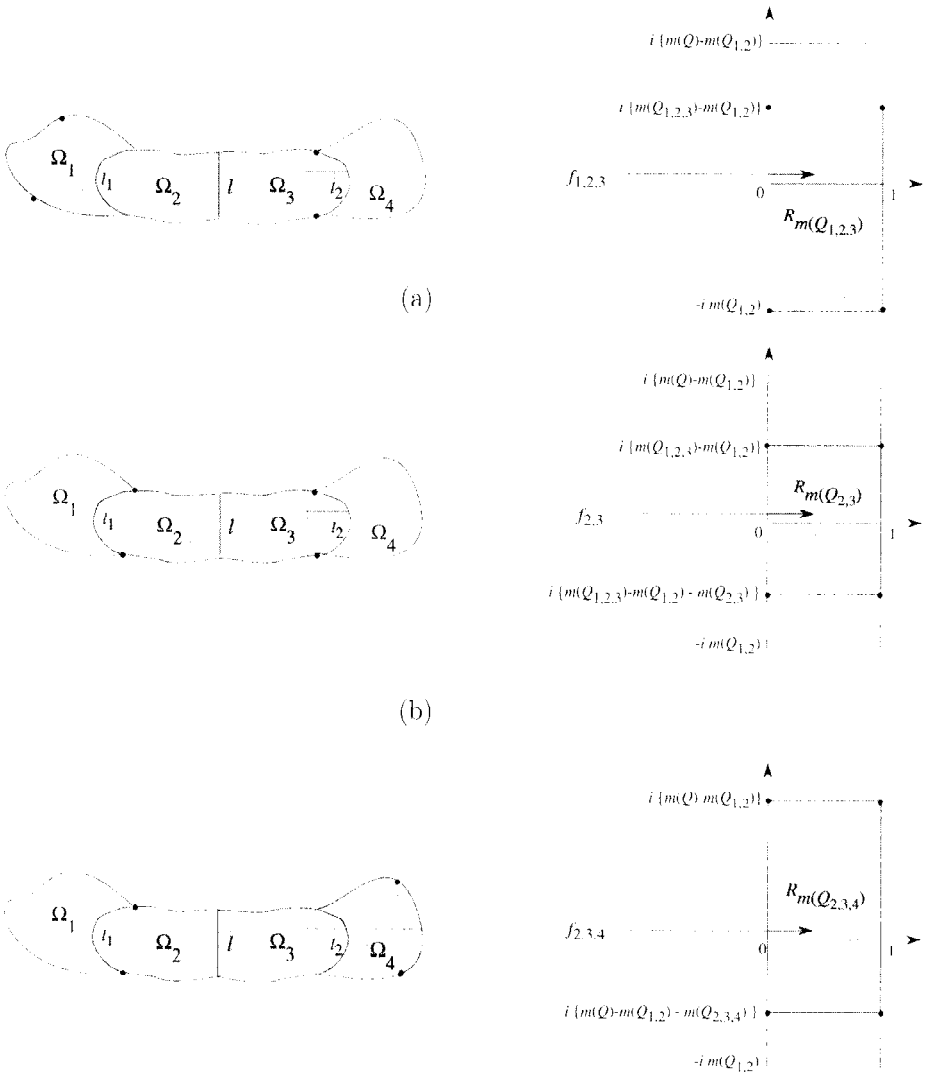

Fig. 3.4

provided $m(Q_2) \geq 1$. Also, if

$$R_{m(Q_2)} := \{(\xi, \eta) : 0 < \xi < 1,\ H_1 < \eta < H_2\},$$

with

$$H_1 := m(Q_{1,2,3}) - m(Q_{1,2}) - m(Q_{2,3}) \quad \text{and} \quad H_2 := m(Q_{1,2,3}) - m(Q_{1,2}) - m(Q_3),$$

then, because of the symmetry of $\Omega_{2,3}$:

$$f_{2,3}(z) = f_2(z), \qquad z \in \Omega_2,$$

where $f_2 : \Omega_2 \to R_{m(Q_2)}$. Therefore, if

$$\alpha := m(Q) - \{m(Q_{1,2,3}) + m(Q_{2,3,4}) - m(Q_{2,3})\},$$

then by using (3.2):

$$\begin{aligned} \max_{z\in\overline{\Omega}_2} |\, f_{2,3,4}(z) - f_{2,3}(z)| &\le \max_{z\in\overline{\Omega}_2} |\, f_{2,3,4}(z) - f_2(z) - i\alpha| + |\alpha| \\ &\le 4.08 e^{-\pi m(Q_2)} + |\alpha|, \end{aligned} \tag{3.17}$$

provided $m(Q_2) \ge 1$. (The quantity α was introduced in the above estimate because the function $f_{2,3,4}$ maps the domain $\Omega_{2,3,4}$ onto the rectangle $R_{m(Q_{2,3,4})}$ whose lower side is at a distance $m(Q) - m(Q_{1,2}) - m(Q_{2,3,4})$, rather than $m(Q_{1,2,3}) - m(Q_{1,2}) - m(Q_{2,3})$, from the real axis; see Figures 3.4(b), (c).) Hence, from (3.15)–(3.17):

$$E_g^{\{2\}} \le 6.12 e^{-\pi m(Q_2)} + |\alpha|, \tag{3.18}$$

provided $m(Q_2) \ge 1$.

(iii)

$$\begin{aligned} E_g^{\{3\}} &= \max_{z\in\overline{\Omega}_3} |\, f_{1,2,3}(z) + f_{2,3,4}(z) - f_{2,3}(z) - f_{3,4}(z)| \\ &\le \max_{z\in\overline{\Omega}_3} |\, f_{1,2,3}(z) - f_{2,3}(z)| + \max_{z\in\overline{\Omega}_3} |\, f_{2,3,4}(z) - f_{3,4}(z) - i\varepsilon_m| + \varepsilon_m, \end{aligned}$$

where the quantity

$$\varepsilon_m := m(Q) - \{m(Q_{1,2}) + m(Q_{3,4})\}$$

is introduced because the function $f_{2,3,4}$ maps the domain $\Omega_{2,3,4}$ onto the rectangle $R_{m(Q_{2,3,4})}$ whose top side is at a distance $m(Q) - m(Q_{1,2})$, rather than $m(Q_{3,4})$, from the real axis; see Figure 3.4(c). Hence, by recognizing that

$$f_{2,3}(z) = f_3(z), \qquad z \in \Omega_3,$$

with

$$f_3 : \Omega_3 \to R_{m(Q_3)} := \{(\xi, \eta) : 0 < \xi < 1,\ H_2 < \eta < m(Q_{1,2,3}) - m(Q_{1,2})\},$$

we obtain from (3.1) and (3.2) that

$$E_g^{\{3\}} \le 6.12 e^{-\pi m(Q_2)} + \varepsilon_m, \tag{3.19}$$

provided $m(Q_2) \ge 1$.

(iv) As in (iii) above, by using (3.1):

$$\begin{aligned} E_g^{\{4\}} &= \max_{z\in\overline{\Omega}_4} |\, f_{2,3,4}(z) - f_{3,4}(z)| \le \max_{z\in\overline{\Omega}_4} |\, f_{2,3,4}(z) - f_{3,4}(z) - i\varepsilon_m| + \varepsilon_m \\ &\le 2.04 e^{-\pi m(Q_2)} + \varepsilon_m, \end{aligned} \tag{3.20}$$

provided $m(Q_2) \ge 1$.

Thus, from (3.13), (3.14), and (3.18)–(3.20):

$$E_f \le \max_{z\in\overline{\Omega}} |f(z)-g(z)| + \max_{z\in\overline{\Omega}} |g(z)-\tilde{f}(z)|, \tag{3.21}$$
$$\le 10.39e^{-2\pi m(Q_2)} + \max_{z\in\overline{\Omega}} |g(z)-\tilde{f}(z)|,$$

where

$$|g(z)-\tilde{f}(z)| \le \begin{cases} 2.04e^{-\pi m(Q_2)} & \text{for } z\in\overline{\Omega}_1, \\ 6.12e^{-\pi m(Q_2)}+|\alpha| & \text{for } z\in\overline{\Omega}_2, \\ 6.12e^{-\pi m(Q_2)}+\varepsilon_m & \text{for } z\in\overline{\Omega}_3, \\ 2.04e^{-\pi m(Q_2)}+\varepsilon_m & \text{for } z\in\overline{\Omega}_4. \end{cases} \tag{3.22}$$

Finally, if $m(Q_2)\ge 1.5$, then Theorems 2.5 and 2.6 of [19] give

$$|\alpha| \le 2.71e^{-2\pi m(Q_2)} \qquad \text{and} \qquad 0\le\varepsilon_m\le 5.26e^{-2\pi m(Q_2)}. \tag{3.23}$$

These, in conjunction with (3.21) and (3.22), yield the required estimate

$$E_f \le 6.17e^{-\pi m(Q_2)}. \qquad \blacksquare$$

Remark 3.2. We note the following regarding the various DDM estimates involved in the proof of Theorem 3.2:

(i) For the two boundary errors

$$E_{\gamma_1} := \max_{z\in\gamma_1} |f(z)-f_{1,2}(z)| \qquad \text{and} \qquad E_{\gamma_2} := \max_{z\in\gamma_2} |f(z)-f_{3,4}(z)|$$

(see Figure 3.3) the following estimates hold:

$$E_{\gamma_1} \le 3.64e^{-\pi m(Q_{1,2,3})} \quad \text{and} \quad E_{\gamma_2} \le 3.64e^{-\pi m(Q_{2,3,4})} + 5.26e^{-2\pi m(Q_2)}, \tag{3.24}$$

provided $m(Q_2)\ge 1.5$. This emerges from (2.33), (2.34), (3.9), (3.23), and the triangle inequalities

$$E_{\gamma_1} \le \max_{z\in\gamma_1} |f(z)-f_{1,2,3}(z)| + \max_{z\in\gamma_1} |f_{1,2,3}(z)-f_{1,2}(z)|, \tag{3.25}$$

$$E_{\gamma_2} \le \max_{z\in\gamma_2} |f(z)-f_{2,3,4}(z)| + \max_{z\in\gamma_2} |f_{2,3,4}(z)-f_{3,4}(z)-i\varepsilon_m| + \varepsilon_m. \tag{3.26}$$

(ii) Since $m(Q_{1,2,3})\ge 2m(Q_2)$ and $m(Q_{2,3,4})\ge 2m(Q_2)$, it follows from (3.24) that the DDM errors on the boundary segments γ_1, γ_2 satisfy

$$E_{\gamma_j} = \mathcal{O}(e^{-2\pi m(Q_2)}), \qquad j=1,2. \tag{3.27}$$

These should be compared with: (a) the orders of the DDM errors on the crosscut of decomposition l, i.e.,

$$E_l^{\{j\}} = \mathcal{O}(e^{-\pi m(Q_2)}), \qquad j=1,2, \tag{3.28}$$

where

$$E_l^{\{1\}} := \max_{z\in l} |f(z) - f_{1,2}(z)|, \qquad E_l^{\{2\}} := \max_{z\in l} |f(z) - f_{3,4}(z)|;$$

(b) with the order of the error of the DDM approximation to the conformal module, i.e.,

$$\varepsilon_m = m(Q) - \{m(Q_{1,2}) + m(Q_{3,4})\} = \mathcal{O}(e^{-2\pi m(Q_2)}) \tag{3.29}$$

(see (3.12) and (3.23)).

(iii) In (3.27) and (3.28) the indicated orders are best possible. For (3.28), this follows from [12, §7], and for (3.27) from the sharpness of the order of the estimate for ε_m (see [5, Theorem 5]), because

$$E_{\gamma_2} \geq |f(z_4) - f_{3,4}(z_4)| = |i\{m(Q) - m(Q_{1,2})\} - im(Q_{3,4})| = \varepsilon_m.$$

4. Numerical Examples

In this section we present three numerical examples illustrating the application of the DDM results obtained in Section 3. Our objectives are as follows:

1. To compare the theoretical estimates for the errors given by (3.12) and (3.24) with the actual DDM errors. We do this in Example 4.1, by considering a polygonal domain for which we can find reliable approximations to the various conformal maps involved in the decomposition.
2. To illustrate how the DDM can be used in conjunction with the MATLAB Schwarz–Christoffel Toolbox (SC Toolbox) of Driscoll [2],[1] for the efficient computation of the conformal mapping of complicated polygonal quadrilaterals (Example 4.2).
3. To present an example where, due to the effects of crowding, the conformal mapping software that we have available can only approximate the conformal map through the use of domain decomposition (Example 4.3).

Example 4.1. We consider the decomposition illustrated in Figure 4.1 and compute approximations to the three conformal maps $f : \Omega \to R_{m(Q)}$, $f_{1,2} : \Omega_{1,2} \to R_{m(Q_{1,2})}$, and $f_{3,4} : \Omega_{3,4} \to R_{m(Q_{3,4})}$ by means of the *conventional method*, i.e., by using the unit disk D as intermediate canonical domain. For this we use:

(a) the double precision version of the integral equation conformal mapping package CONFPACK of Hough [10][2] to compute the conformal map of the defining domain of each quadrilateral onto the unit disk;

(b) the subroutine `wsc` of the Schwarz–Christoffel package SCPACK of Trefethen [20], [21] to compute, in each case, the inverse Jacobian elliptic sine that takes D onto the associated rectangle.

[1] The SC Toolbox can be obtained from: http://amath-www.colorado.edu/appm/faculty/tad/.

[2] The double precision version of CONFPACK has only become available recently; see http://www.mis.coventry. ac.uk/∼dhough/.

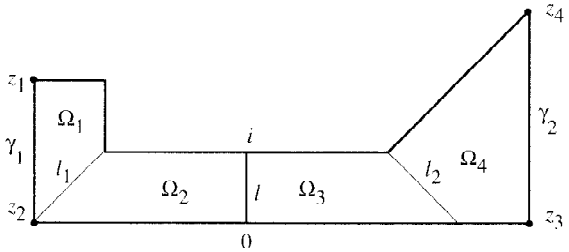

Fig. 4.1. The coordinates of the special points, starting from z_1 and moving in counterclockwise order, are $(-k-1.,2.)$, $(-k-1.,0.)$, $(k+2.,0.)$, $(k+2.,3.)$.

(Although SCPACK is known to be robust for the computation of the mapping from the unit disk onto the polygon, the package has not been designed for the efficient computation of the mapping onto the unit disk; see [21, p. 17]. For this reason, for mapping onto D, we prefer to use CONFPACK.)

Regarding accuracy, we expect that the computed approximations to the functions f, $f_{1,2}$, and $f_{3,4}$ (and to the associated conformal modules $m(Q)$, $m(Q_{1,2})$, and $m(Q_{3,4})$) are correct to at least eight decimal places. This can be deduced, as described in [4, p. 188], by taking into account the CONFPACK error estimates for the conformal maps onto the unit disk (which are all less than 2.6×10^{-12}) and the measures of crowding.

In presenting the numerical results we employ the following notations:

- $E_l^{\{j\}}$ and E_{γ_j}, $j = 1, 2$: These denote the "actual" DDM errors:

$$E_{\gamma_1} := \max_{z\in\gamma_1} |f(z) - f_{1,2}(z)|, \qquad E_l^{\{1\}} := \max_{z\in l} |f(z) - f_{1,2}(z)|,$$

  and

$$E_{\gamma_2} := \max_{z\in\gamma_2} |f(z) - f_{3,4}(z)|, \qquad E_l^{\{2\}} := \max_{z\in l} |f(z) - f_{3,4}(z)|,$$

  which are determined from the "accurate" CONFPACK approximations to the functions f, $f_{1,2}$, and $f_{3,4}$, by sampling the error functions $f(z) - f_{1,2}(z)$ and $f(z) - f_{3,4}(z)$ at an appropriate number of test points on γ_1, γ_2, and l.
- $T(E_l^{\{j\}})$ and $T(E_{\gamma_j})$, $j = 1, 2$: These denote, respectively, the theoretical estimates for the errors $E_l^{\{j\}}$ and E_{γ_j} given by Theorem 3.2 and Remark 3.2(i), i.e.,

$$T(E_l^{\{j\}}) := 6.17e^{-\pi m(Q_2)}, \qquad j = 1, 2, \tag{4.1}$$

  and

$$T(E_{\gamma_1}) := 3.64e^{-\pi m(Q_{1,2,3})}, \qquad T(E_{\gamma_2}) := 3.64e^{-\pi m(Q_{2,3,4})} + 2.56e^{-2\pi m(Q_2)}. \tag{4.2}$$

- $\delta(E_l^{\{j\}})$ and $\delta(E_{\gamma_j})$, $j = 1, 2$: These denote the values used for testing the validity of the predicted orders

$$E_l^{\{j\}} = \mathcal{O}(e^{-\pi m(Q_2)}) \quad \text{and} \quad E_{\gamma_j} = \mathcal{O}(e^{-2\pi m(Q_2)}), \qquad j = 1, 2, \tag{4.3}$$

Table 4.1. Values of conformal modules.

k	$m(Q_2)$	$m(Q_{1,2,3})$	$m(Q_{2,3,4})$
1.00	1.279 261 571	3.011 339 976	3.580 314 206
1.25	1.529 343 037	3.511 418 502	4.080 380 646
1.50	1.779 359 959	4.011 434 815	4.580 394 450
1.75	2.029 363 477	4.511 438 206	5.080 397 319
2.00	2.229 364 208	5.011 438 911	5.580 397 915

of the errors $E_l^{\{j\}}$ and E_{γ_j}; see (3.28) and (3.27). They are determined from the computed values of $E_l^{\{j\}}$ and E_{γ_j} by:

(a) assuming that

$$E(k) \approx Ce^{-\delta\pi m(k)},$$

where $E(k)$ stands for any of the errors $E_l^{\{j\}}$, E_{γ_j}, corresponding to the dimension parameter k of the quadrilateral Q, δ stands for the order $\delta(E_l^{\{j\}})$ or $\delta(E_{\gamma_j})$, and $m(k)$ denotes the conformal module of the quadrilateral Q_2, corresponding to the parameter k;

(b) computing the various values of δ by means of the formula

$$\delta = -\{\log[E(k_1)/E(k_2)]\}/\{\pi(m(k_1) - m(k_2))\},$$

where k_1 and k_2 are taken to be successive values of the parameter k for which numerical results are listed.

(Therefore, from the theory, we expect to obtain values $\delta(E_l^{\{j\}}) \approx 1$ and $\delta(E_{\gamma_j}) \approx 2$, $j = 1, 2$.)

The numerical results corresponding to the values $k = 1.00(0.25)\ 2.00$ are listed in Tables 4.1, 4.2, and 4.3. Table 4.1 contains the values of the auxiliary conformal modules $m(Q_2)$, $m(Q_{1,2,3})$, and $m(Q_{2,3,4})$, which are needed for the DDM error analysis (see Theorem 3.2 and (4.1)–(4.2)). These were computed by means of the subroutine `resist` of SCPACK and are expected to be correct to all the figures quoted.

The results listed in Tables 4.2 and 4.3 illustrate the high accuracy that can be achieved by domain decomposition (even when the quadrilaterals involved are only moderately elongated) and confirm nicely the predicted orders of approximation given by (4.3). In particular, we note that the numerical results display the predicted order of approximation even in the case $k = 1$, for which $m(Q_2)$ does not satisfy the requirement $m(Q_2) \geq$

Table 4.2. Errors and orders in approximating f by $f_{1,2}$.

k	$E_l^{\{1\}}$	$T(E_l^{\{1\}})$	$\delta(E_l^{\{1\}})$	E_{γ_1}	$T(E_{\gamma_1})$	$\delta(E_{\gamma_1})$
1.00	4.3e-4	*	—	3.7e-6	*	—
1.25	1.9e-4	5.0e-2	1.01	7.6e-7	5.8e-5	2.00
1.50	8.8e-5	2.3e-2	1.00	1.6e-7	1.2e-5	2.00
1.75	4.0e-5	1.0e-2	1.00	3.3e-8	2.5e-6	2.00
2.00	1.8e-5	5.6e-3	1.00	6.9e-9	5.3e-7	2.00

Table 4.3. Errors and orders in approximating f by $f_{3,4}$.

k	$E_I^{\{2\}}$	$T(E_I^{\{2\}})$	$\delta(E_I^{\{2\}})$	E_{γ_2}	$T(E_{\gamma_2})$	$\delta(E_{\gamma_2})$
1.00	4.3e-4	*	—	8.3e-7	*	—
1.25	1.9e-4	5.0e-2	1.01	1.7e-7	1.8e-4	2.00
1.50	8.8e-5	2.3e-2	1.00	3.6e-8	3.8e-5	2.00
1.75	4.0e-5	1.0e-2	1.00	1.2e-8	7.8e-6	**
2.00	1.8e-5	5.6e-3	1.00	1.2e-8	2.2e-6	**

1.5 needed for our error analysis. This indicates that the assumption $m(Q_2) \geq 1.5$ in Theorem 3.2 might be somewhat pessimistic. (In fact, we know that the condition can be relaxed somewhat, but at the cost of increasing the constants in the error estimates; see, e.g., Lemma 2.1(i).) We also note that, since the overall accuracy of the mapping f is of the order 10^{-8}, the "actual" error E_{γ_2} does not improve beyond 1.2×10^{-8}. Because of this, we cannot compute meaningful values of $\delta(E_{\gamma_2})$ in the two cases $k = 1.75$ and $k = 2$.

Example 4.2. Consider the quadrilateral $Q := \{\Omega; z_1, z_2, z_3, z_4\}$ of Figure 4.2, where the width of each strip of the spiral Ω is 1, and the special points z_1, z_2, z_3, z_4, of Q are, respectively, the four (outermost and innermost) corners $19+18i$, $18+18i$, $9+9i$, $10+9i$ of Ω. The mapping of the above quadrilateral was first considered by Howell and Trefethen in [11], for the purpose of illustrating the performance of a modified Schwarz–Christoffel technique for elongated quadrilaterals. The mapping was also studied in [16],

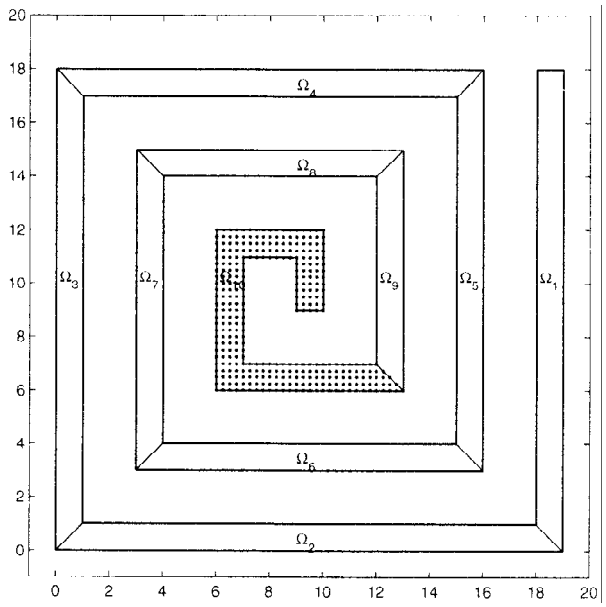

Fig. 4.2. The decomposition of Q and a grid of points on $\overline{\Omega}_{10}$.

[17], and [18], in connection with the use of the DDM for computing conformal modules. In particular, the estimate

$$132.704\,539\,3 < m(Q) < 132.704\,540\,3$$

was obtained in [18, p. 276].

Here, we consider again the mapping of Q, in order to illustrate the substantial gain in computational efficiency that can be achieved when the conformal mapping package SC Toolbox of Driscoll [2] is used in conjunction with the DDM. We note that the SC Toolbox contains a subroutine (subroutine `crrectmap`), which is capable of computing the conformal modules and the corresponding conformal maps of elongated polygonal quadrilaterals. This is done by employing the cross-ratios and Delaunay triangulation technique of Driscoll and Vavasis [3], for overcoming the crowding difficulties associated with the conformal mapping onto the unit disk. (It should be noted that this technique of [3] requires the introduction of a number of additional auxiliary vertices on the sides of the defining polygon.) For the particular quadrilateral Q of Figure 4.2, `crrectmap` requires a CPU time of more than 3.5 hours, in order to compute approximations (with estimated accuracy 1.66×10^{-7}) to $m(Q)$ and to the parameters that define the mapping function $f : \Omega \to R_{m(Q)}$.

For the application of the DDM, we decompose Q as illustrated in the figure and determine DDM approximations to $m(Q)$ and f, by applying the subroutine `crrectmap` to each component quadrilateral. That is:

(a) we use `crrectmap` for computing $m(Q_j)$ and $f_j : \Omega_j \to R_{m(Q_j)}$, $j = 1, \ldots, 10$, where the rectangles $R_{m(Q_j)}$ are given by (1.2)–(1.3);
(b) we approximate $m(Q)$ and f by means of

$$\widetilde{m}(Q) := \sum_{j=1}^{10} m(Q_j) \tag{4.4}$$

and

$$\widetilde{f}(z) := f_j(z), \qquad z \in \Omega_j, \quad j = 1, \ldots, 10. \tag{4.5}$$

The DDM numerical results obtained are listed in Table 4.4, together with those that correspond to applying `crrectmap` directly to Q. The meaning of the notations is as follows:

- N: This denotes the total number of vertices (ordinary and auxiliary) used by `crrectmap` for the computation of the corresponding mapping.
- Time I: This denotes the CPU time, in seconds, needed for the setting up of the auxiliary vertices and for the computation of the parameters that define the conformal map.
- Time II: This denotes the CPU time, in seconds, needed for the mapping of a 0.25×0.25 grid of points from the quadrilateral under consideration onto the associated rectangle. (The images of the grid corresponding to the component quadrilateral Q_{10} are shown in Figure 4.3.)
- m: This denotes the computed value of the conformal module of the quadrilateral under consideration.

Table 4.4. Direct versus DDM application of `crrectmap`.

	N	Time I	Time II	m
Q	136	12686	447	132.704 540
Q_1	20	69	29	17.279 364
Q_2	20	68	29	17.558 729
Q_3	20	70	26	16.558 729
Q_4	20	58	23	14.558 729
Q_5	20	55	21	13.558 729
Q_6	14	70	20	11.558 729
Q_7	8	49	26	10.558 729
Q_8	8	28	19	8.558 729
Q_9	8	23	15	7.558 729
Q_{10}	16	100	35	14.955 345
Sum	154	590	243	132.704 540

All computations were carried out on an IBM RS 6000/360 workstation, using MATLAB 5.3. In all cases, the SC Toolbox estimate of accuracy of the computed approximations was between 2.0×10^{-8} and 3.0×10^{-7}.

As is shown in Table 4.4, the direct computation of the conformal map f by means of `crrectmap` requires a CPU time of more that 3.5 hours. By contrast, the computation of f by means of (4.4)–(4.5) (using the DDM in conjunction with `crrectmap`) requires a

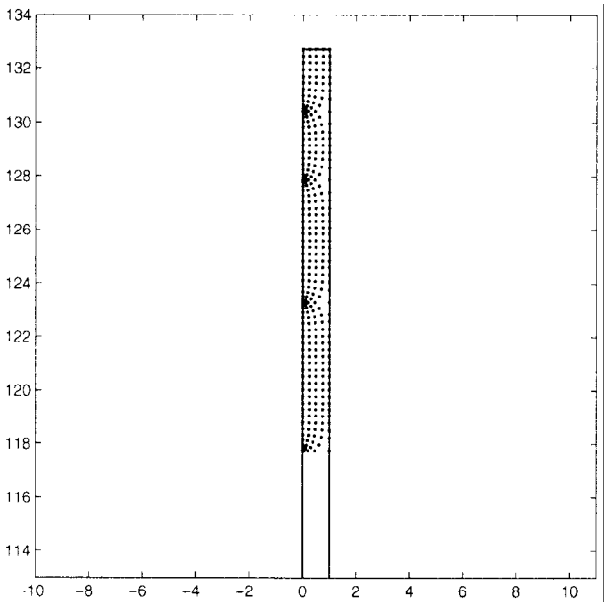

Fig. 4.3. The images of the grid points shown in Figure 4.2 on the (partly shown) conformally equivalent rectangle.

CPU time of less than 10 minutes. In other words, the use of DDM leads to a substantial reduction in CPU time, by a factor of about $\frac{1}{20}$. (Clearly, the reduction in time will be even more substantial in a parallel computing environment.) Furthermore, once the conformal map is determined, the use of the DDM for the mapping of the grid points leads to a further reduction in CPU time, by a factor of about $\frac{1}{2}$.

The error analysis for the DDM approximations (4.4) and (4.5) can be performed by the repeated use of Theorems 3.1, 3.2, and [19, Theorems 2.4, 2.6]; see, e.g., the DDM error analysis in [17, Example 3.2]. This leads to the following estimates:

$$0 < m(Q) - \widetilde{m}(Q) \leq 3.60 \times 10^{-15} \qquad \text{and} \qquad \max_{z \in \overline{\Omega}} |f(z) - \widetilde{f}(z)| \leq 1.61 \times 10^{-7}.$$

Thus, since the direct application of `crrectmap` led to approximations of accuracy 1.66×10^{-7}, we can conclude that the substantial reduction in computational time was achieved by the DDM at no cost in the overall accuracy.

We end this section by presenting an example that involves a quadrilateral, for which the software that we have available can approximate the corresponding conformal map only through the use of the DDM.

Example 4.3. Consider the quadrilateral $Q := \{\Omega; z_1, z_2, z_3, z_4\}$ of Figure 4.4, where the width of each of the arms that form Ω is 1, and the two boundary arcs γ_1 and γ_2 are given, respectively, by

$$\gamma_1 := \{(x, y) : x = 0.25y^4 - 0.5y^2 + 7,\ 0 \leq y \leq 1\}$$

and

$$\gamma_2 := \{(x, y) : x = 7.5 + 0.25\cos(2\pi(9 - y)),\ 9 \leq y \leq 10\}.$$

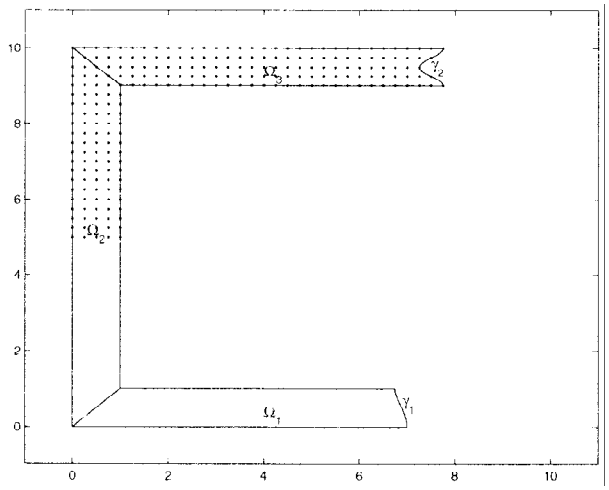

Fig. 4.4. The decomposition of Q and a grid of points on $\overline{\Omega}$.

In this case, the available software cannot be used to compute $f : \Omega \to R_{m(Q)}$ directly, because:

(a) due to the curved boundary arcs γ_1 and γ_2, the SC Toolbox of Driscoll cannot be employed;
(b) due to severe crowding, the use of the conventional method in conjunction with CONFPACK breaks down completely.

(With reference to (b), the CONFPACK estimate for the error of the conformal map onto the unit disk is 2.3×10^{-12}. However, because of severe crowding the computer fails to recognize the images of the special points z_1, z_2, z_3, z_4, in the correct order on the unit circle; see the discussion about crowding in [13, §3.1], and observe that, as can be seen by inspection, $m(Q) > 20$.)

For the application of the DDM, we decompose Q as illustrated in the figure, and determine approximations to $m(Q)$ and f, by applying the conventional method, in conjunction with CONFPACK and the subroutine `wsc` of SCPACK, to each of the component quadrilaterals Q_j, $j = 1, 2, 3$. That is:

(a) we use CONFPACK and `wsc`, in exactly the same way as in Example 4.1, for computing $m(Q_j)$ and $f_j : \Omega_j \to R_{m(Q_j)}$, $j = 1, 2, 3$, where the rectangles $R_{m(Q_j)}$ are given by (1.2)–(1.3);
(b) we approximate $m(Q)$ and f by means of

$$\widetilde{m}(Q) := \sum_{j=1}^{3} m(Q_j) \tag{4.6}$$

and

$$\widetilde{f}(z) := f_j(z), \quad z \in \Omega_j, \quad j = 1, 2, 3. \tag{4.7}$$

With reference to (a), CONFPACK and `wsc` lead to approximations which are expected to be correct to at least nine decimal places. This is deduced from the CONFPACK error estimates for the conformal maps onto the unit disk (which are all less than 8.0×10^{-14}) and the measures of crowding. In particular, the computed values of $m(Q_j)$, $j = 1, 2, 3$, are given, correct to nine decimal places, by

$$m(Q_1) = 6.138\,933\,434, \qquad m(Q_2) = 8.558\,728\,798, \qquad m(Q_3) = 6.643\,454\,032. \tag{4.8}$$

The error analysis for the DDM approximations (4.6) and (4.7) can be performed by the repeated use of [19, Theorem 2.4], for determining the error in $\widetilde{m}(Q)$, and by the repeated use of Theorem 3.1, for the error in $\widetilde{f}$. This leads to the following estimates:

$$0 < m(Q) - \widetilde{m}(Q) \le 2.36 \times 10^{-17} \qquad \text{and} \qquad \max_{z \in \overline{\Omega}} |f(z) - \widetilde{f}(z)| \le 1.72 \times 10^{-8}.$$

Thus, by recalling the error in the CONFPACK/`wsc` approximations, we can conclude that:

(a) $m(Q)$ is given by (4.6) correct to eight decimal places by

$$m(Q) = 21.341\,116\,26;$$

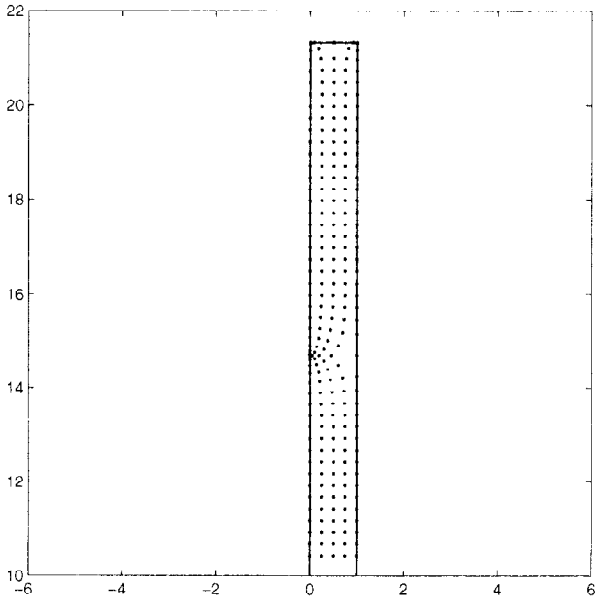

Fig. 4.5. The images of the grid points, shown in Figure 4.4, on the (partly shown) conformally equivalent rectangle.

(b) Equation (4.7) produces an approximation to the conformal map f, which is correct to at least seven decimal places. The images of a 0.25×0.25 grid of points, that cover a part of Ω, onto the rectangle $R_{m(Q)}$, are shown in Figure 4.5.

References

1. L. V. AHLFORS (1973): Conformal Invariants: Topics in Geometric Function Theory. McGraw-Hill Series in Higher Mathematics. New York: McGraw-Hill.
2. T. A. DRISCOLL (1996): *Algorithm* 657: *A MATLAB toolbox for Schwarz–Christoffel mapping*. ACM Trans. Math. Soft., **22**:168–186.
3. T. A. DRISCOLL, S. A. VAVASIS (1998): *Numerical conformal mapping using cross-ratios and Delaunay triangulation*. SIAM J. Sci. Comput., **19**:1783–1803.
4. M. I. FALCÃO, N. PAPAMICHAEL, N. S. STYLIANOPOULOS (1999): *Curvilinear crosscuts of subdivision for a domain decomposition method in numerical conform mapping*. J. Comput. Appl. Math., **106**:177–196.
5. D. GAIER, W. K. HAYMAN (1990): *Moduli of long quadrilaterals and thick ring domains*. Rend. Math. Appl. (7), **10**:809–834.
6. D. GAIER, W. K. HAYMAN (1991): *On the computation of modules of long quadrilaterals*. Constr. Approx., **7**:453–467.
7. D. GAIER, N. PAPAMICHAEL (1987): *On the comparison of two numerical methods for conformal mapping*. IMA J. Numer. Anal., **7**:261–282.
8. W. K. HAYMAN (1948): *Remarks on Ahlfors' distortion theorem*. Quart. J. Math. (Oxford), **19**:33–53.
9. P. HENRICI (1986): Applied and Computational Complex Analysis, Vol. III. New York: Wiley.
10. D. M. HOUGH (1990): User's Guide to CONFPACK. IPS Research Report 90-11, ETH-Zentrum. CH-8092 Zurich, Switzerland.
11. L. H. HOWELL, L. N. TREFETHEN (1990): *A modified Schwarz–Christoffel transformation for elongated regions*. SIAM J. Sci. Statist. Comput., **11**:928–949.

12. R. LAUGESEN (1994): *Conformal mapping of long quadrilaterals and thick doubly connected domains*. Constr. Approx., **10**:523–554.
13. N. PAPAMICHAEL (1989): *Numerical conformal mapping onto a rectangle with applications to the solution of Laplacian problems*. J. Comput. Appl. Math., **28**:63–83.
14. N. PAPAMICHAEL, N. S. STYLIANOPOULOS (1990): *On the numerical performance of a domain decomposition method for conformal mapping*. In: Computational Methods and Function Theory 1989, St. Ruscheweyh (E. B. Saff, L. C. Salinas, R. S. Varga, eds.). Lecture Notes in Mathematics, Vol. 1435, pp. 155–169. Berlin: Springer-Verlag.
15. N. PAPAMICHAEL, N. S. STYLIANOPOULOS (1991): *A domain decomposition method for conformal mapping onto a rectangle*. Constr. Approx., **7**:349–379.
16. N. PAPAMICHAEL, N. S. STYLIANOPOULOS (1992): *A domain decomposition method for approximating the conformal modules of long quadrilaterals*. Numer. Math., **62**:213–234.
17. N. PAPAMICHAEL, N. S. STYLIANOPOULOS (1994): *On the theory and application of a domain decomposition method for computing conformal modules*. J. Comput. Appl. Math., **50**:33–50.
18. N. PAPAMICHAEL, N. S. STYLIANOPOULOS (1995): *Domain decomposition for conformal maps*. In: Computational Methods and Function Theory 1994 (R. M. Ali, St. Ruscheweyh, E. B. Saff, eds.), Ser. Approx. Decompos., Vol. 5, pp. 267–291. River Edge, NJ: World Scientific.
19. N. PAPAMICHAEL, N. S. STYLIANOPOULOS (1999): *The asymptotic behavior of conformal modules of quadrilaterals with applications to the estimation of resistance values*. Constr. Approx., **15**:109–134.
20. L. N. TREFETHEN (1980): *Numerical computation of the Schwarz–Christoffel transformation.* SIAM J. Sci. Statist. Comput., **1**:82–102.
21. L. N. TREFETHEN (1989): SCPACK User's Guide. Numerical Analysis Report 89-2, Department of Mathematics, MIT. Cambridge, MA.

M. I. Falcão
Centro de Matemática
Universidade do Minho
Campus de Gualtar
4700 Braga
Portugal
mif@math.uminho.pt

N. Papamichael
Department of Mathematics and Statistics
University of Cyprus
PO Box 20537
CY-1678 Nicosia
Cyprus
nickp@ucy.ac.cy

N. S. Stylianopoulos
Department of Mathematics and Statistics
University of Cyprus
PO Box 20537
CY-1678 Nicosia
Cyprus
nikos@ucy.ac.cy